

The compatibility of LHC Run 1 data with a heavy scalar of mass around 270 GeV

Stefan von Buddenbrock^a, Nabarun Chakrabarty^b, Alan S. Cornell^c, Deepak Kar^a, Mukesh Kumar^c, Tanumoy Mandal^b, Bruce Mellado^a, Biswarup Mukhopadhyaya^b, Robert G. Reed^a

^a*School of Physics, University of the Witwatersrand, Johannesburg, Wits 2050, South Africa*

^b*Regional Centre for Accelerator-based Particle Physics, Harish-Chandra Research Institute, Chhatnag Road, Jhusi, Allahabad - 211 019, India.*

^c*National Institute for Theoretical Physics; School of Physics and Mandelstam Institute for Theoretical Physics, University of the Witwatersrand, Johannesburg, Wits 2050, South Africa*

Abstract

The first run of the LHC was successful in that it saw the discovery of the elusive Higgs boson, a particle that is consistent with the SM hypothesis. There are a number of excesses in Run 1 ATLAS and CMS results which can be interpreted as being due to the existence of another heavier scalar particle. This particle has decay modes which we have studied using LHC Run 1 data. Using a minimalistic model, we can predict the kinematics of these final states and compare the prediction against data directly. A statistical combination of these results shows that a best fit point is found for a heavy scalar having a mass of 272_{-9}^{+12} GeV. This result has been quantified as a three sigma effect, based on analyses which are not necessarily optimized for the search of a heavy scalar. The smoking guns for the discovery of this new heavy scalar and the prospects for Run 2 are discussed.

Keywords: Higgs boson, Heavy scalar, Dark matter

PACS: 14.80.Bn, 14.80.Ec, 12.60.Cn, 12.60.Fr

1. Introduction

With the discovery of a new scalar boson (which will be denoted by h) at the Large Hadron Collider (LHC) [1, 2], new tasks and explorations have come to the fore. Both the ATLAS and CMS experiments have been keenly exploring the properties of the new scalar, and will continue to do so in the high-energy run(s). This includes tests on various coupling strengths as well as spin-CP properties. Overall, the global fits of the data indicate that the properties are mostly consistent with what the Standard Model (SM) of particle physics expects for a Higgs boson. Nonetheless, there are certain features and excesses in the available data that warrant detailed attention. Table 1 summarizes the measurements made by the ATLAS and CMS experiments that are considered here. These results comprise the measurements of the differential Higgs boson transverse momentum (p_{T_h}) (where h is the SM-like Higgs.), searches for a di-Higgs boson resonance, the Higgs boson in association with top quarks, and VV resonances (where $V = Z, W^\pm$). These final states are considered against the hypothesis of a heavy scalar boson (H).

In order to describe the shape of the p_{T_h} distribution, it is necessary to introduce decays in which at least one h is produced: $H \rightarrow hh, h\chi\chi$ where χ would be a dark matter candidate, leading to the production of the Higgs boson in association with missing energy. The latter could be realized through the decay of some intermediate particle. This hypothetical intermediate particle (the existence or nature of which we make no statement about) could also decay into a pair of light hadronic jets. In either case, a distortion of the p_{T_h} spectrum would be expected.

Both ATLAS and CMS have observed excesses in the production of a SM Higgs boson in association with top quarks. The new boson would naturally be produced in association with top quarks. In addition, with a small branching ratio to VV , the effect of negative interference in single top associated production is suppressed, and we would expect a large cross section for a heavy scalar being produced in association with top quarks. These effects would yield an explanation for the excesses which are seen in the data.

While none of the excesses summarized in Table 1 is significant enough on its own, it is tantalizing to study their compatibility as a whole with the decay of one new heavy boson. In fact, viewed under this hypothesis, the overall size of the excess could be significant. We adopt a bottom-up approach and wait for an overseeing theory until the observed results are further consolidated. The fit of the available data presented here by us will hopefully enable people to put all pieces of the jigsaw puzzle

Email addresses: stef.von.b@cern.ch (Stefan von Buddenbrock), nabarunc@hri.res.in (Nabarun Chakrabarty), Alan.Cornell@wits.ac.za (Alan S. Cornell), Deepak.Kar@cern.ch (Deepak Kar), mukesh.kumar@cern.ch (Mukesh Kumar), tanumoymandal@hri.res.in (Tanumoy Mandal), Bruce.Mellado@wits.ac.za (Bruce Mellado), biswarup@hri.res.in (Biswarup Mukhopadhyaya), Robert.Reed@cern.ch (Robert G. Reed)

Result	Publication	
Differential Higgs boson p_T spectra	ATLAS	Fiducial cross section measurements on $h \rightarrow \gamma\gamma$ [3] and $h \rightarrow ZZ^* \rightarrow 4\ell$ [4]
	CMS	Fiducial cross section measurements on $h \rightarrow \gamma\gamma$ [5] and $h \rightarrow ZZ^* \rightarrow 4\ell$ [6]
Di-Higgs boson resonance searches	ATLAS	Limits on $H \rightarrow hh \rightarrow b\bar{b}\tau\tau$, $\gamma\gamma WW^*$, $\gamma\gamma b\bar{b}$ and $b\bar{b}b\bar{b}$ [7]
	CMS	Limits on $H \rightarrow hh \rightarrow \gamma\gamma b\bar{b}$ [8], $b\bar{b}\tau\tau$ [9] and multi-lepton [10]
Top associated Higgs boson production	ATLAS	Limits on $h \rightarrow \gamma\gamma$ [11] Measurements on multi-lepton decay channels [12] and $h \rightarrow b\bar{b}$ [13]
	CMS	Measurements on $h \rightarrow \gamma\gamma$, $h \rightarrow b\bar{b}$ and multi-lepton decay channels [14]
$H \rightarrow VV$ decays	ATLAS	Limits on $H \rightarrow WW$ [15] and ZZ [16]
	CMS	Limits on $H \rightarrow WW$ and ZZ [17]

Table 1: A list of the experimental results which were used to help constrain the relevant parameters of the proposed model. In the interest of being as unbiased as possible, these results were selected regardless of whether they hint at physics beyond the SM.

together once a larger volume of results accumulates. It is important to note that some of the experimental analyses used in this study were not optimized for the search of a heavy scalar boson. Therefore, the sensitivity to the search is not maximized, rendering conservative the results reported here.

The salient features of the suggested scenario are summarised in Section 2. In Sections 3 and 4 the main tools of our analysis are discussed with Section 3 focussed on the statistical machinery used. The results are presented and discussed in Section 5 including a discussion on smoking guns and prospects for Run 2, followed by a brief conclusion in Section 6.

2. A suggested scenario

The features and excesses which are seen in the data have been treated in such a way that they could be explained purely by physics beyond the SM (BSM). We propose a scenario which is a BSM extension to the SM, allowing us to write

$$\mathcal{L} = \mathcal{L}_{\text{SM}} + \mathcal{L}_{\text{BSM}}, \quad (1)$$

where all of the new interactions and states are encoded in \mathcal{L}_{BSM} .

The simplest approach is to treat the new interactions as arising from effective couplings. We have assumed h to have SM interactions with fermions and gauge bosons. The sectors of the proposed BSM Lagrangian involving the new scalars (omitting the usual mass and kinetic energy terms) include,

$$\mathcal{L}_{\text{BSM}} \supset \mathcal{L}_H + \mathcal{L}_Y + \mathcal{L}_T + \mathcal{L}_Q, \quad (2)$$

where terms \mathcal{L}_Y , \mathcal{L}_T and \mathcal{L}_Q are the Yukawa, trilinear and quartic interactions relevant for this study, respectively. These sectors are defined as follows,

$$\mathcal{L}_H = -\frac{1}{4} \beta_g \kappa_{hgg}^{\text{SM}} G_{\mu\nu} G^{\mu\nu} H + \beta_V \kappa_{hVV}^{\text{SM}} V_\mu V^\mu H, \quad (3)$$

$$\mathcal{L}_Y = -\frac{1}{\sqrt{2}} \left[y_{ttH} \bar{t}tH + y_{bbH} \bar{b}bH \right], \quad (4)$$

$$\mathcal{L}_T = -\frac{1}{2} v \left[\lambda_{Hhh} Hhh + \lambda_{h\chi\chi} h\chi\chi + \lambda_{H\chi\chi} H\chi\chi \right], \quad (5)$$

$$\begin{aligned} \mathcal{L}_Q = & -\frac{1}{2} \lambda_{Hh\chi\chi} Hh\chi\chi - \frac{1}{4} \lambda_{HHhh} HHhh \\ & - \frac{1}{4} \lambda_{hh\chi\chi} hh\chi\chi - \frac{1}{4} \lambda_{HH\chi\chi} HH\chi\chi, \end{aligned} \quad (6)$$

where H and χ denote the heavy scalar and the DM candidate respectively (the latter is assumed to be a scalar for illustration), and $v = 246$ GeV is the vacuum expectation value that is responsible for the W - and Z -boson masses. This can be looked upon as a variant of Higgs boson portal scenarios [18, 19, 20]. This Lagrangian could in principle emerge as an effective theory after electroweak symmetry breaking in any gauge-invariant extended scalar sector. The second term in Eq. (3) is summed over the weak vector bosons Z and W^\pm , and the κ factors are the SM-like couplings, with $\kappa_{hgg}^{\text{SM}} = \alpha_s/(3\pi v)$ and $\kappa_{hVV}^{\text{SM}} \simeq m_V^2/v$.

We deliberately make no statement about the gauge quantum numbers carried by H , but just postulate that the above terms stay after electroweak symmetry breaking. We set $\beta_g \kappa_{hgg}^{\text{SM}}$ to be the strength of the effective gluon-gluon coupling of H . In situations where there are no additional effects over and above the top-mediated triangle diagrams contributing to this effective interaction, $\beta_g = y_{ttH}/y_{ttH}^{\text{SM}}$ where y_{ttH}^{SM} is the SM top Yukawa coupling. There would also be a similar relation for the bottom Yukawa coupling y_{bbH} , but this has been counted as negligible since the effect of bottom quarks in gluon fusion loops is small. The production of H is made to occur through gluon fusion and its rate can therefore be controlled by varying β_g . Likewise, the HVV couplings can be tuned by varying β_V .

It should again be remembered that we are not making any definite statement on the origin of each term. Thus, as we shall see below, the $Hh\chi\chi$ (effective) coupling is required to be on the high side, keeping the observed data in mind. We do not rule out the possibility of this being due to the participation of some real particle in the

intermediate state, as discussed above.

Major constraints on the Lagrangian parameters stem from the observations of the relic density of DM [21] and the DM-nuclei inelastic scattering cross sections [22]. These constraints are controlled by the two model parameters m_χ and $\lambda_{h\chi\chi}$. It is found that both of these DM constraints can simultaneously be satisfied for a narrow choice of the parameters $m_\chi \sim [55 - 60]$ GeV for very small $\lambda_{h\chi\chi} \sim [0.0006 - 0.006]$ [23]. This keeps the invisible decay width of h well within the observed limits. Other model couplings remain unconstrained by these observations.

Within this simplistic framework, one expects the process $pp \rightarrow H \rightarrow h\chi\chi$ to generate an enhanced p_T , owing to the fact that h now recoils against a pair of invisible particles. The presence of a $H\chi\chi$ coupling opens the potential for detecting invisible decays following the methodology suggested in Ref. [24].

3. Statistical formalism

The BSM prediction constructed using the proposed model was fit against four classes of constraints. The constraints considered are differential Higgs boson p_T spectra, the limits on di-Higgs boson production through a resonance, various limits and measurements on top associated Higgs boson production, and the limits on a heavy scalar decaying to vector bosons. For each class of constraints, results from both ATLAS and CMS were used to avoid bias. These results are summarized in Table 1. A simultaneous fit was done in terms of calculating and minimising a combined χ^2 value while varying β_g for different m_H hypotheses. Statistically, two types of results were dealt with: measurements and limits.

A calculation of χ^2 for a measurement is straightforward. Given a measurement μ with its associated error $\Delta\mu$, one can construct a χ^2 by testing the measurement against a theoretical prediction and its associated theoretical uncertainty, given as μ^{th} and $\Delta\mu^{\text{th}}$, respectively. The uncertainties from the measurement and the theoretical prediction are assumed to be independent and are added up in quadrature, allowing us to calculate the χ^2 as

$$\chi^2 = \frac{(\mu - \mu^{\text{th}})^2}{(\Delta\mu)^2 + (\Delta\mu^{\text{th}})^2}. \quad (7)$$

To calculate a χ^2 from a result in the form of a 95% confidence limit (CL), we need only assume that given some measurement μ with its expected and observed limits μ^{exp} and μ^{obs} respectively, the χ^2 is Gaussian in μ . Then, assuming the null hypothesis has $\mu = 0$, we can extract the mean of the distribution as $\mu^{\text{obs}} - \mu^{\text{exp}}$. This is treated as the excess in μ which can be tested against a theoretical prediction μ^{th} . Its error is inserted as $\Delta\mu = \mu^{\text{exp}}/1.96$, where the 1.96 arises from the fact that 95% confidence corresponds to 1.96 units of standard deviation in a Gaussian distribution – this approach is used in Ref. [25] and

other references therein. Using this, the χ^2 is calculated as

$$\chi^2 = \frac{(\mu^{\text{obs}} - \mu^{\text{exp}} - \mu^{\text{th}})^2}{(\mu^{\text{exp}}/1.96)^2}. \quad (8)$$

Using the definitions in Eqs. (7) and (8), a combined χ^2 was constructed by adding up the contributions from all of the results presented in Table 1. This procedure is described in the following section.

4. Methodology and tools

The minimal model we have described was built first using `FeynRules` [26] and then passed to the Universal FeynRules Output [27] such that event generation could be performed at leading order (LO) in `MadGraph5` [28]. Computations relating to DM constraints in the model were carried out using `micrOMEGAs` [29].

Fitting the ATLAS and CMS Higgs boson p_T spectra with the BSM prediction was accomplished as follows. Events with the $h\chi\chi$ and hh final states were generated from pp collisions through an H s -channel in `MadGraph5` and showered appropriately using `PYTHIA 8.2` [30]. Since the ATLAS [3, 4] and CMS [5, 6] Higgs boson p_T spectra were constructed from fiducial volumes of phase space, it was important that BSM prediction went through the same event selection. This was done using the `Rivet` [31] analysis framework. The total LO cross section of the BSM prediction was enhanced to NNLL+NLO (next-to-next-to-leading log plus next-to-leading order accuracy) through multiplication by an appropriately calculated k-factor determined from Ref. [32].

The BSM prediction was tested against the SM-only prediction. For the SM, fiducial acceptance factors for gluon fusion (ggF) are given in Refs. [3, 4, 5, 6]. The ggF Higgs boson p_T prediction was generated at NLO using `MinLO HJ` [33]. This prediction was further reweighted to NNLO accuracy and scaled to the NNLL+NLO cross section from Ref. [32]. The other less prominent Higgs boson production modes (VBF, Vh and $t\bar{t}h$, which are collectively referred to as Xh) were taken directly from the ATLAS and CMS publications.

The bulk of the production cross section is in the intermediate p_{T_h} range where ggF is the dominant production mode. In this mechanism, QCD radiative corrections play a critical role in generating p_{T_h} . The Monte Carlo (MC) used to simulate ggF describes the p_{T_h} distribution at NNLL+NLO. Recent results on the NNLO corrections on ggF+1j production indicate that, although moderate, corrections are still significant [34, 35]. NNLO corrections with respect to NLO can be as large as 25% in the range of interest. In order to accommodate these corrections, a conservative approach is implemented. The p_{T_h} distribution with $p_{T_h} > 30$ GeV is corrected with the NNLO/NLO k-factors provided in Ref. [34]. The MC described is normalized to the total ggF cross section at NNLO. The first

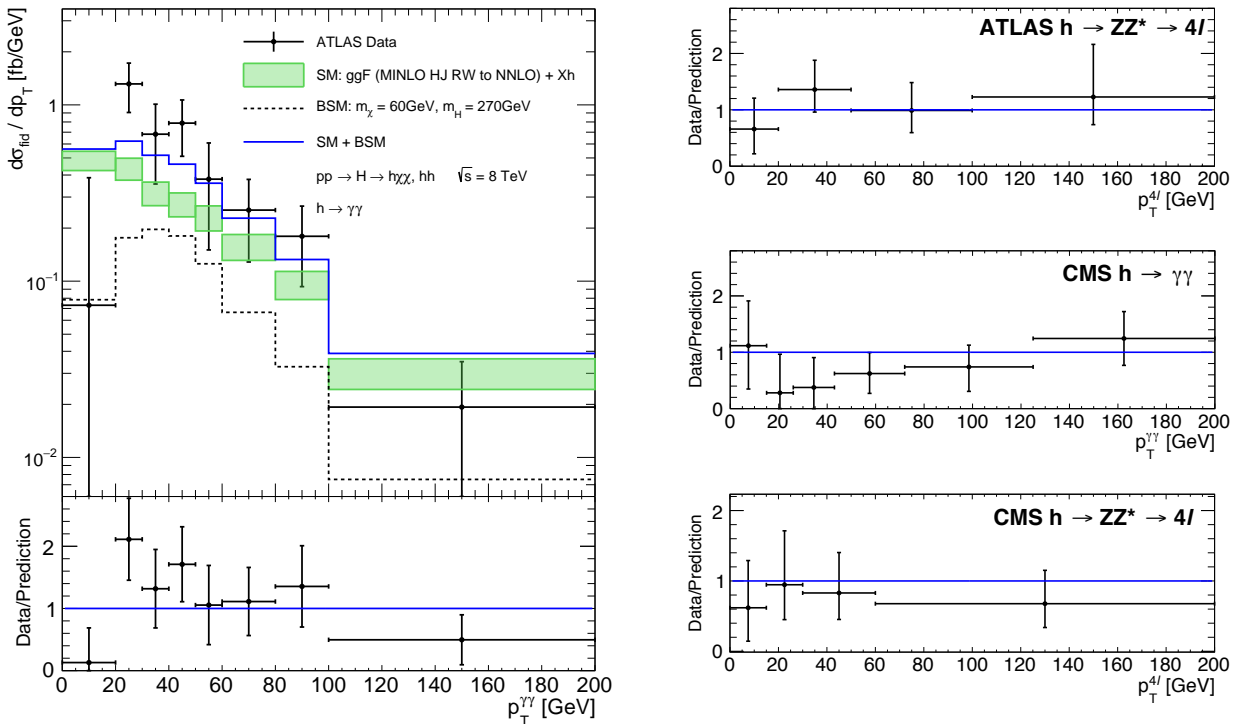


Figure 1: Fits to the fiducial differential distributions of the Higgs boson transverse momentum using the ATLAS diphoton [3] (left), the ATLAS $h \rightarrow ZZ^* \rightarrow 4\ell$ [4] (top right), the CMS diphoton [5] (middle right) and CMS $h \rightarrow ZZ^* \rightarrow 4\ell$ [6] (bottom right) decays (see text for detailed description). The mass points considered here are the best fit values of $m_\chi = 60$ GeV and $m_H = 270$ GeV. In the interest of saving space, only one full plot has been shown, with the other three are plots of a ratio between the data and BSM prediction.

complete calculation of the total ggF cross section at N³LO is now available and it is indicative of small N³LO/NNLO k-factors and scale variations [36]. For this reason the cross section with $p_{Th} < 30$ GeV is re-scaled appropriately so that the total cross section does not exceed the total cross section by more than 2% with respect to the calculation at NNLO. The scale uncertainties assumed in this analysis remain at NNLO for the total cross section and at NLO for the p_{Th} , while the PDF uncertainties were conservatively taken from Ref. [32]. Other production mechanisms of the SM Higgs boson do not play a critical role in the region of the phase-space under study, and were therefore left unmodified. A similar approach is taken for the BSM prediction. The p_T of the heavy scalar is reweighted by determining a reweighting function from an NLO calculation using OneLOoP [37] in MG5_aMC@NLO [38] compared to the result obtained with the shower. Overall, the shower does a reasonable job, matching the LO prediction within 20%. The effect of the these corrections on the transverse momentum of the Higgs boson from the decay of H is small and it reduces to a positive shift of about 3 GeV. It is, however, important to note that the jet multiplicity of the H boson in this setup is significantly larger than that characteristic to h . This implies a significant reduction of the jet veto survival probability.

Excesses in top associated Higgs boson production were also included in the fits. Associated th production in the

SM is suppressed due to the negative interference induced by the relative sign of the Yukawa and hWW couplings (see Ref. [39] and other references therein). If the hWW coupling is relatively suppressed, this negative interference is reduced, so that its cross section becomes comparable to that of ttH production. For this reason, β_V was set to a small value (order of 10^{-3}) and tH cross sections were determined at LO in MadGraph5. These cross sections were enhanced to NNLL+NLO by multiplying by an appropriate k-factor, and were then combined with ttH cross sections from Ref. [32]. For the mass values of the heavy scalar considered in this analysis (between 260 and 320 GeV) the combined cross section from tH and ttH reached a value as high as 25 fb at $\sqrt{s} = 8$ TeV.

The statistical combination was done using the techniques described in Section 3. Firstly, the branching ratios of $H \rightarrow hh$ and $H \rightarrow VV$ were fixed by minimising a χ^2 determined from experimental results. These branching ratios were used as inputs for a combined χ^2 , which was calculated while floating the free parameters β_g and m_H . For each mass point, β_g was marginalised such that the combined χ^2 was minimised. Errors on marginalised parameters were calculated from identifying the points in parameter space which differ by one unit of χ^2 above and below the minimised value.

5. Results and discussion

In this analysis the global χ^2 is minimized for different m_H hypotheses. The technical part of the analysis was done using a scan of mass points, starting at $m_H = 260$ GeV and going up in 5 GeV steps until 320 GeV. Points in between these were reached by an interpolation. The other parameters of the model are fixed by a number of constraints. Firstly, the branching ratio of $H \rightarrow hh$ is set to a value that is best fit against the current di-Higgs boson resonance search limits set by ATLAS and CMS. Secondly, the branching ratio of $H \rightarrow VV$ is determined in the same way using ATLAS and CMS limits from searches for $H \rightarrow VV$ at high masses. The remainder of the decay of the heavy scalar is assumed to be $H \rightarrow h\chi\chi$. Finally, the parameter β_g is constrained by fitting the ATLAS and CMS Higgs boson p_T spectra, as well as excesses in top associated Higgs boson production. There may exist other decay modes, such as $H \rightarrow \chi\chi$. The invisible decay is not considered here. Adding in other decay modes would not change the final results of the analysis, although it would allow us to further constrain the parameter β_g .

Calculating and minimising the χ^2 described in Sections 3 and 4, it was found that the lower values of m_H fit the experimental data better than the higher values. Out of the mass points considered, the $m_H = 270$ GeV point was able to minimise the χ^2 value the most. This point was determined using the best fit values of the branching ratios as $\text{BR}(H \rightarrow hh) = 0.030 \pm 0.037$, $\text{BR}(H \rightarrow ZZ) = 0.025 \pm 0.018$ and $\text{BR}(H \rightarrow WW) = 0.057 \pm 0.041$. The parameter β_g was best fit at the value of 1.5 ± 0.6 . The errors on these quantities correspond to a 1σ deviation from the mean value. An indication of this parameter fitting the ATLAS and CMS p_T spectra can be seen in Fig. 1. The fits to the p_T spectra were also able to constrain the mass of the DM candidate; for $m_H = 270$ GeV, m_χ was best fit at 60 GeV. This is very close to $m_h/2$, which naturally leads to the suppression of the branching ratio of $h \rightarrow \chi\chi$, and it is consistent with current direct search limits. The distribution with the filled band corresponds to the prediction made by the SM. The width of the band indicates the size of the uncertainties on the ggF process, according to the conservative scheme discussed in Section 4. These uncertainties are incorporated in the χ^2 . The dotted line shows the contribution from $H \rightarrow h\chi\chi$ as well as $H \rightarrow hh$. The solid line corresponds to the sum of the SM and BSM components.

When interpolating between mass points, the combined minimised χ^2 is found to be smallest at the value $m_H = 272$ GeV, with upper and lower errors being 12 GeV and 9 GeV, respectively. This can be seen in Fig. 2 where the solid blue line shows the lowest value of the minimised χ^2 , and the dotted blue lines show a 1σ deviation from the value. The minimised value of χ^2 has a lowest value of 0.72 per degree of freedom in the fit. It should be noted here that when comparing the BSM hypothesis to a null hypothesis (the SM with a 125 GeV Higgs boson), the im-

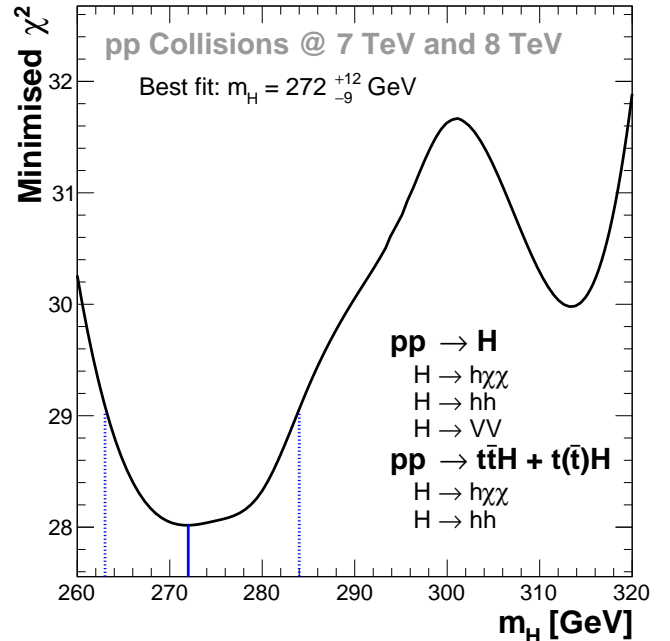


Figure 2: A scan of minimised χ^2 values as a function of the free parameter m_H . This was constructed by minimising an additive χ^2 with contributions from all of the experimental results in Table 1. These results were compared to the BSM prediction described mostly in Section 4.

provement on explaining experimental data just surpasses a 3σ effect at the best fit point, as can be seen in Fig. 3. In this figure, the large significance around $m_H = 260$ GeV can be attributed to the large $pp \rightarrow H \rightarrow hh$ cross sections in most of the ATLAS and CMS di-Higgs boson resonance search results. It is also relevant to note that results reported here do not change significantly if the NNLO corrections on ggF+1j discussed in the previous section are not applied.

The most immediate consequence of the phenomenological model considered here is the appearance of intermediate missing transverse energy in association with h . In addition, data appears to display more jets in association to h than expected in the SM. This applies both to the inclusive production and the production in association with top quarks. Enhanced QCD radiation in the production of H compared to that of direct h production may not be sufficient to explain the effect. As a result, one can also consider the decay of the hypothetical intermediate particle (discussed in Section 1) into hadronic jets. These effects would lead to an enhanced jet multiplicity in the inclusive production of h as well as in association with top quarks. This also opens the opportunity for a resonant structure in the hjj spectrum.

In the light of this discussion, presented below is a list of possible smoking guns for investigation with Run 2 data:

- Higgs boson in association with moderate and large

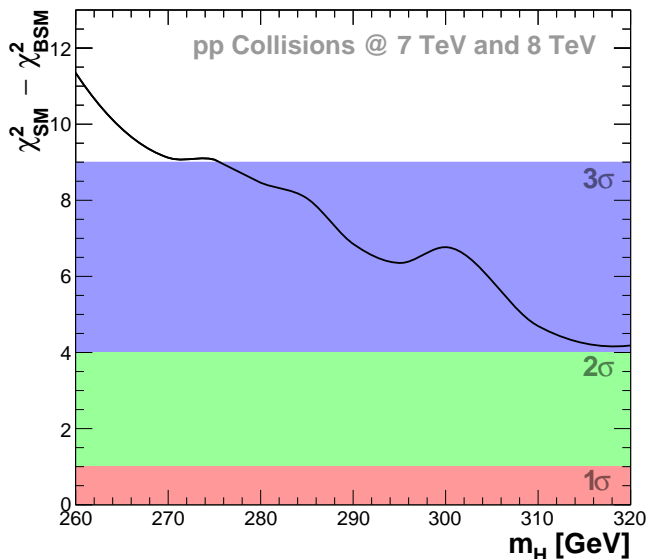


Figure 3: A scan over m_H of the test statistic $\chi_{\text{SM}}^2 - \chi_{\text{BSM}}^2$ employed for quantifying the significance of the effect of the BSM model. The 1σ , 2σ and 3σ bands for one degree of freedom are shown in red, green and blue, respectively. The SM hypothesis corresponds to the existence of the SM Higgs boson, but the complete absence of the heavy scalar (i.e. the $pp \rightarrow H$ cross section is set to 0).

missing energy.

- Higgs boson in association with at least two hadronic jets, including a resonant structure in the hjj spectrum.
- Higgs boson in association with top quarks and large missing energy (greater than 100 GeV)
- Higgs boson in association with top quarks and at least two additional hadronic jets, including a resonant structure in the hjj spectrum.
- Resonant structure in the VV invariant mass spectrum.
- Resonant structure in the hh invariant mass spectrum.
- Missing energy recoiling against a high transverse momentum jet.

It is beyond the scope of this paper to quantify the amount of integrated luminosity required for the ATLAS and CMS experiments to declare a 5σ effect. However, it is noted that the design of dedicated data analysis will greatly enhance the sensitivity reached with the available results from Run 1 studied here.

6. Conclusions

ATLAS and CMS data results comprising measurement of the differential Higgs boson transverse momentum, searches for a di-Higgs boson resonance, the Higgs

boson in association with top quarks, and VV resonances, have been considered against the hypothesis of a heavy scalar. The analysis yields a best fit result with a 3σ effect. The hypothetical heavy boson mass is measured to be 272_{-9}^{+12} GeV. In this setup the heavy scalar would predominantly decay into at least one Higgs boson in association with missing energy or hadronic jets. These results are obtained on the basis of analyses that are not optimized for the search of the heavy scalar discussed here. It is expected that dedicated optimizations will significantly enhance the sensitivity to the search. A number of final states have been identified that can serve as smoking guns for the discovery of the heavy scalar discussed here.

Acknowledgements

The work of N.C., T.M. and B. Mukhopadhyaya was partially supported by funding available from the Department of Atomic Energy, Government of India for the Regional Centre for Accelerator-based Particle Physics (RECAPP), Harish-Chandra Research Institute. B. Mellado acknowledges the hospitality of RECAPP during the collaboration. The Claude Leon Foundation are acknowledged for their financial support. The High Energy Physics group of the University of the Witwatersrand is grateful for the support from the Wits Research Office, the National Research Foundation, the National Institute of Theoretical Physics and the Department of Science and Technology through the SA-CERN consortium and other forms of support.

References

References

- [1] G. Aad *et al.* (ATLAS Collaboration), *Phys. Lett.* **B716**, 1 (2013), [arXiv:1207.7214 \[hep-ex\]](#).
- [2] S. Chatrchyan *et al.* (CMS Collaboration), *Phys. Lett.* **B716**, 30 (2012), [arXiv:1207.7235 \[hep-ex\]](#).
- [3] G. Aad *et al.* (ATLAS Collaboration), *JHEP* **09**, 112 (2014), [arXiv:1407.4222 \[hep-ex\]](#).
- [4] G. Aad *et al.* (ATLAS Collaboration), *Phys. Lett.* **B738**, 234 (2014), [arXiv:1408.3226 \[hep-ex\]](#).
- [5] V. Khachatryan *et al.* (CMS Collaboration), (2015), [arXiv:1508.07819 \[hep-ex\]](#).
- [6] CMS Collaboration, (2015), CMS-PAS-HIG-14-028.
- [7] G. Aad *et al.* (ATLAS Collaboration), (2015), [arXiv:1509.04670 \[hep-ex\]](#).
- [8] CMS Collaboration, (2014), CMS-PAS-HIG-13-032.
- [9] V. Khachatryan *et al.* (CMS Collaboration), (2015), [arXiv:1510.01181 \[hep-ex\]](#).
- [10] V. Khachatryan *et al.* (CMS Collaboration), *Phys. Rev.* **D90**, 112013 (2014), [arXiv:1410.2751 \[hep-ex\]](#).
- [11] G. Aad *et al.* (ATLAS Collaboration), *Phys. Lett.* **B740**, 222 (2015), [arXiv:1409.3122 \[hep-ex\]](#).
- [12] G. Aad *et al.* (ATLAS Collaboration), *Phys. Lett.* **B749**, 519 (2015), [arXiv:1506.05988 \[hep-ex\]](#).
- [13] G. Aad *et al.* (ATLAS Collaboration), *Eur. Phys. J.* **C75**, 349 (2015), [arXiv:1503.05066 \[hep-ex\]](#).
- [14] V. Khachatryan *et al.* (CMS Collaboration), *JHEP* **09**, 087 (2014), [Erratum: *JHEP*10,106(2014)], [arXiv:1408.1682 \[hep-ex\]](#).

- [15] G. Aad *et al.* (ATLAS Collaboration), (2015), [arXiv:1509.00389 \[hep-ex\]](#) .
- [16] G. Aad *et al.* (ATLAS Collaboration), (2015), [arXiv:1507.05930 \[hep-ex\]](#) .
- [17] V. Khachatryan *et al.* (CMS Collaboration), (2015), [arXiv:1504.00936 \[hep-ex\]](#) .
- [18] W.-L. Guo and Y.-L. Wu, *JHEP* **10**, 083 (2010), [arXiv:1006.2518 \[hep-ph\]](#) .
- [19] Y. Cai, X.-G. He, and B. Ren, *Phys. Rev.* **D83**, 083524 (2011), [arXiv:1102.1522 \[hep-ph\]](#) .
- [20] M. Gonderinger, H. Lim, and M. J. Ramsey-Musolf, *Phys. Rev.* **D86**, 043511 (2012), [arXiv:1202.1316 \[hep-ph\]](#) .
- [21] P. A. R. Ade *et al.* (Planck), *Astron. Astrophys.* **571**, A16 (2014), [arXiv:1303.5076 \[astro-ph.CO\]](#) .
- [22] D. S. Akerib *et al.* (LUX), *Phys. Rev. Lett.* **112**, 091303 (2014), [arXiv:1310.8214 \[astro-ph.CO\]](#) .
- [23] J. M. Cline, K. Kainulainen, P. Scott, and C. Weniger, *Phys. Rev.* **D88**, 055025 (2013), [Erratum: *Phys. Rev.* D92,no.3,039906(2015)], [arXiv:1306.4710 \[hep-ph\]](#) .
- [24] A. Djouadi, A. Falkowski, Y. Mambrini, and J. Quevillon, *Eur. Phys. J.* **C73**, 2455 (2013), [arXiv:1205.3169 \[hep-ph\]](#) .
- [25] P. P. Giardino, K. Kannike, I. Masina, M. Raidal, and A. Strumia, *JHEP* **05**, 046 (2014), [arXiv:1303.3570 \[hep-ph\]](#) .
- [26] A. Alloul, N. D. Christensen, C. Degrande, C. Duhr, and B. Fuks, *Comput. Phys. Commun.* **185**, 2250 (2014), [arXiv:1310.1921 \[hep-ph\]](#) .
- [27] C. Degrande, C. Duhr, B. Fuks, D. Grellscheid, O. Mattelaer, and T. Reiter, *Comput. Phys. Commun.* **183**, 1201 (2012), [arXiv:1108.2040 \[hep-ph\]](#) .
- [28] J. Alwall, M. Herquet, F. Maltoni, O. Mattelaer, and T. Stelzer, *JHEP* **06**, 128 (2011), [arXiv:1106.0522 \[hep-ph\]](#) .
- [29] G. Belanger, F. Boudjema, A. Pukhov, and A. Semenov, *Comput. Phys. Commun.* **185**, 960 (2014), [arXiv:1305.0237 \[hep-ph\]](#) .
- [30] T. Sjostrand, S. Ask, J. R. Christiansen, R. Corke, N. Desai, P. Ilten, S. Mrenna, S. Prestel, C. O. Rasmussen, and P. Z. Skands, *Comput. Phys. Commun.* **191**, 159 (2015), [arXiv:1410.3012 \[hep-ph\]](#) .
- [31] A. Buckley, J. Butterworth, L. Lonnblad, D. Grellscheid, H. Hoeth, J. Monk, H. Schulz, and F. Siegert, *Comput. Phys. Commun.* **184**, 2803 (2013), [arXiv:1003.0694 \[hep-ph\]](#) .
- [32] J. R. Andersen *et al.* (LHC Higgs Cross Section Working Group), (2013), 10.5170/CERN-2013-004, [arXiv:1307.1347 \[hep-ph\]](#) .
- [33] K. Hamilton, P. Nason, and G. Zanderighi, *JHEP* **10**, 155 (2012), [arXiv:1206.3572 \[hep-ph\]](#) .
- [34] R. Boughezal, F. Caola, K. Melnikov, F. Petriello, and M. Schulze, *Phys. Rev. Lett.* **115**, 082003 (2015), [arXiv:1504.07922 \[hep-ph\]](#) .
- [35] R. Boughezal, C. Focke, W. Giele, X. Liu, and F. Petriello, *Phys. Lett.* **B748**, 5 (2015), [arXiv:1505.03893 \[hep-ph\]](#) .
- [36] C. Anastasiou, C. Duhr, F. Dulat, F. Herzog, and B. Mistlberger, *Phys. Rev. Lett.* **114**, 212001 (2015), [arXiv:1503.06056 \[hep-ph\]](#) .
- [37] A. van Hameren, *Comput. Phys. Commun.* **182**, 2427 (2011), [arXiv:1007.4716 \[hep-ph\]](#) .
- [38] J. Alwall, R. Frederix, S. Frixione, V. Hirschi, F. Maltoni, O. Mattelaer, H. S. Shao, T. Stelzer, P. Torrielli, and M. Zaro, *JHEP* **07**, 079 (2014), [arXiv:1405.0301 \[hep-ph\]](#) .
- [39] M. Farina, C. Grojean, F. Maltoni, E. Salvioni, and A. Thamm, *JHEP* **05**, 022 (2013), [arXiv:1211.3736 \[hep-ph\]](#) .